



## REVIEW ARTICLE

# Molecular Imaging of Inflammation and Infection: A Glimpse of the Past and a Look at the Future

Christopher J. Palestro<sup>1\*</sup>, Charito Love<sup>1</sup>, Kuldeep K. Bhargava<sup>1</sup>

<sup>1</sup>Northwell, New Hyde Park, NY, Department of Radiology at Donald and Barbara Zucker School of Medicine at Hofstra/ Northwell, Hempstead, NY and Radiology Long Island Jewish Medical Center, New Hyde Park, NY.

\*[palestro@northwell.edu](mailto:palestro@northwell.edu)



OPEN ACCESS

## PUBLISHED

31 December 2024

## CITATION

Palestro, C.J., Love, C., et al., 2024. Molecular Imaging of Inflammation and Infection: A Glimpse of the Past and a Look at the Future. Medical Research Archives, [online] 12(12).

<https://doi.org/10.18103/mra.v12.i12.6117>

## COPYRIGHT

© 2024 European Society of Medicine. This is an open-access article distributed under the terms of the Creative Commons Attribution License, which permits unrestricted use, distribution, and reproduction in any medium, provided the original author and source are credited.

## DOI

<https://doi.org/10.18103/mra.v12.i12.6117>

## ISSN

2375-1924

## ABSTRACT

Despite significant advances in our understanding of microorganisms and an increased availability of antimicrobial therapy, infection remains a major cause of morbidity and mortality. The diagnosis is not always clearcut and imaging studies often are used for confirmation and localization. For nearly sixty years, molecular imaging has played a significant role in the diagnosis of infection. Bone scintigraphy, for musculoskeletal infections, and gallium-67 (<sup>67</sup>Ga) scintigraphy were the first molecular imaging agents used for diagnosing and localizing infection. There are significant drawbacks to both tests. Bone scintigraphy, though sensitive, lacks specificity, and its role is limited to that of a screening test. Poor imaging characteristics, together with lack of specificity, the 48-72 hour interval between administration and imaging, and limited availability, are significant disadvantages to <sup>67</sup>Ga. Presently <sup>67</sup>Ga is used primarily for differentiating acute tubular necrosis from interstitial nephritis and as an alternative to fluorine-18 fluorodeoxyglucose (<sup>18</sup>F-FDG) for some indications, i.e. sarcoid, spondylodiscitis, and fever of unknown origin, when this agent is not available. The development of a technique to radiolabel leukocytes in vitro and image their accumulation in infection was a watershed event in molecular imaging of infection. In-vitro labeled autologous leukocyte imaging replaced <sup>67</sup>Ga as the molecular imaging test of choice for most infections in immunocompetent individuals and, nearly forty years after its approval in the United States, remains a valuable diagnostic test. Although developed for tumor imaging, <sup>18</sup>F-FDG also accumulates in infection and inflammation. Over the past twenty-five years <sup>18</sup>F-FDG has established itself as a valuable imaging agent for musculoskeletal and cardiovascular infections and as the molecular imaging agent of choice for fever of unknown origin, sarcoid, tuberculosis and spondylodiscitis and has shown promise for monitoring treatment response. Despite their utility, the uptake of these agents depends on the host response to infection, not infection itself. These agents are not infection specific, and investigators have, for many years, sought to develop infection specific agents. Initial attempts such as radiolabeled antibiotics and vitamins met with limited success. More recent investigations with radiolabeled nucleoside analogs, peptides, sugars, and amino acids, are encouraging and hold great promise for the future.

## Introduction

Nearly one hundred years after the discovery of penicillin in 1928, infection still is a major threat to humankind, first in morbidity and third in mortality among all human diseases. As recently as 2017, infection accounted for more than eight million deaths and 400,000 years of life lost<sup>1</sup>. The diagnosis of infection is not always straightforward and imaging studies are frequently included in the diagnostic workup. Radiological studies, like ultrasonography, computed tomography (CT), and magnetic resonance imaging (MRI), identify structural changes produced by a combination of the infection and the host's response to the infection. Functional, or molecular, imaging tests use small quantities, or tracer amounts, of radioactive materials that reflect the physiological changes that are part of the inflammatory process that precede the appearance of structural changes. These agents can be taken up directly by cells, tissues and organs or can be attached to native substances that subsequently migrate to the region of interest. Technetium-99m diphosphonates, for musculoskeletal infections, and gallium-67 citrate, once the mainstays of molecular imaging of infection have largely been replaced by in-vitro labeled leukocytes and fluorine-18 fluorodeoxyglucose. Although useful, these agents

reflect the host response to infection, not the infection itself. Initial attempts at developing infection specific, or at least more specific, molecular imaging agents included radiolabeled antibiotics, antimicrobial peptides and vitamins. More recent investigations have focused on radiolabeled amino acids, nucleoside analogues, sugars, and PET compounds. This manuscript reviews the history of molecular imaging in inflammation and infection and highlights new developments in the field, both for diagnosis and monitoring treatment response.

## The Past

### TECHNETIUM-99M DIPHOSPHONATES

Technetium-99m (<sup>99m</sup>Tc) labeled diphosphonates, typically methylene or hydroxymethylene diphosphonate, are bone seeking agents whose uptake depends on blood flow and rate of new bone formation. Bone scintigraphy, ubiquitously available, relatively inexpensive, and easy to perform, can become positive within two days after the onset of symptoms. The three-phase bone scan, which consists of a perfusion, or flow, phase, blood pool, or tissue, phase and skeletal, or delayed, phase was, for many years, the molecular imaging test of choice for osteomyelitis (Figure 1)<sup>2</sup>.

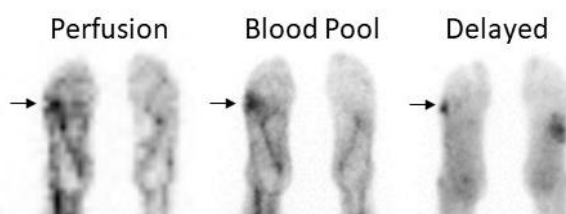


**Figure 1.** Osteomyelitis 5<sup>th</sup> metatarsal right foot. Classic presentation of focal hyperperfusion, hyperemia, and bony uptake (arrows)

The test is extremely accurate in virgin, unviolated bone with sensitivity and specificity more than 90%<sup>3</sup>. Uptake of bone agents, however, is independent of the cause of increased new bone formation, and in the setting of violated bone, specificity decreases. In a review of patients with

underlying bony abnormalities, the 3-phase bone scan was 95% sensitive but only 33% specific<sup>3</sup>. With the advent of advanced imaging tests such as CT, MRI, and labeled leukocytes, the majority of patients referred for bone scintigraphy have underlying osseous abnormalities, i.e. fractures,

orthopedic hardware, etc., and the examination is used primarily as a screening test. While a negative result excludes osteomyelitis with a high degree of certainty, a positive result requires further workup.

#### GALLIUM-67 CITRATE

The first reports about the use of gallium-67 citrate ( $^{67}\text{Ga}$ ) for diagnosing and localizing infection appeared in the early 1970's<sup>4,5</sup>. Although the mechanisms have never been fully elucidated,  $^{67}\text{Ga}$  uptake in infection likely is due to a combination of factors; all of them, however, need not be present for uptake to occur. About 90% of circulating,  $^{67}\text{Ga}$  is transferrin bound in the plasma. Increased blood flow and vascular membrane permeability lead to increased  $^{67}\text{Ga}$  delivery and accumulation at

infectious foci. This radiopharmaceutical is avidly bound to lactoferrin, which is present in sites of infection. Direct bacterial uptake, complexing with siderophores and transport by leukocytes also likely contribute to the uptake of this radiopharmaceutical in infection. Even though some  $^{67}\text{Ga}$  is transported via leukocytes, it is worth mentioning that this agent can detect infection in patients with few or no circulating white cells. Imaging usually is performed 48-72 hours after  $^{67}\text{Ga}$  administration. The normal distribution includes liver, skeleton, gastrointestinal and urinary tracts, and soft tissues, although this is variable and is affected by transfusions, recent surgery and hyperprolactinemic states (Figure 2)<sup>6</sup>.

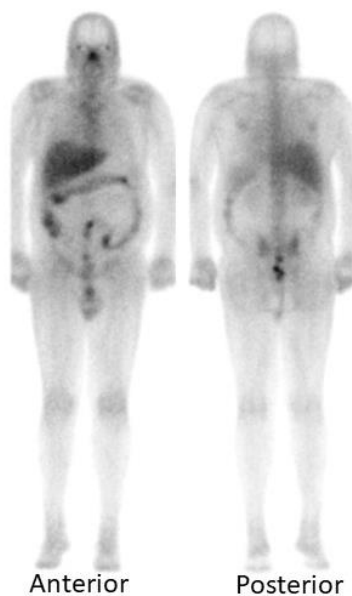


Figure 2. Normal gallium-67 scan (48 hours post injection)

For nearly twenty years, through the late 1980's,  $^{67}\text{Ga}$  was the principal molecular imaging agent for infection and was especially valuable in the initial phase of the HIV/AIDS epidemic. By analyzing pulmonary uptake patterns it was possible to predict with a high degree of certainty whether or not the patient had pneumocystis pneumonia<sup>6</sup>. As clinicians became more familiar with AIDS associated diseases and with the increased sophistication of other imaging modalities, the need for, and use of,  $^{67}\text{Ga}$  imaging in this population all but disappeared.

$^{67}\text{Ga}$  accumulates in tumors, fractures and normally healing surgical incisions in addition to infection.

This lack of specificity along with unfavorable imaging characteristics, the long interval between administration and imaging and the advent of labeled leukocyte imaging and subsequently fluorine-18 fluorodeoxyglucose ( $^{18}\text{F}$ -FDG), hastened its demise. At the present time  $^{67}\text{Ga}$  is used primarily for differentiating acute tubular necrosis from interstitial nephritis in patients with acute renal failure (Figure 3). It also can substitute for  $^{18}\text{F}$ -FDG when the latter is not available, for fever of unknown origin, sarcoid, and spinal infections<sup>7,8</sup>.

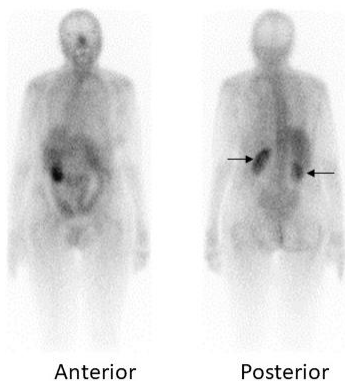


Figure 3. Interstitial nephritis. Compare the renal activity (arrows) in this patient to the renal activity in figure 2 patient.

## The Present

### IN-VITRO LABELED LEUKOCYTES

The development of a technique to radiolabel leukocytes in vitro and image their migration was a watershed event in molecular imaging of infection<sup>9</sup>. In-vitro labeled autologous leukocyte (WBC) imaging, which rapidly replaced <sup>67</sup>Ga as the molecular imaging test of choice for most infections in immunocompetent individuals, remains a valuable diagnostic procedure nearly four decades after its approval in the USA.

Besides intact chemotaxis, WBC uptake depends on the number and types of leukocytes labeled, as well as the cellular response to the infection. A total circulating white blood cell count of at least 2000/uL is needed to obtain satisfactory images. In the usual clinical milieu, most leukocytes labeled are neutrophils, so the test is most sensitive for detecting neutrophil-mediated inflammatory processes, such as bacterial infections. Labeled

leukocyte imaging is less sensitive for detecting inflammatory processes in which the predominant cellular response is not neutrophilic, such as tuberculosis, sarcoid and opportunistic infections<sup>10</sup>. It is important to be cognizant of the fact that although WBC imaging is not specific for infection, it is specific for leukocyte mediated inflammatory processes, and will be positive in any neutrophil mediated inflammatory process, e.g, rheumatoid arthritis<sup>10</sup>.

The in-vitro labeling of leukocytes, which takes about 3 hours, can be performed with either indium-111 oxine (<sup>111</sup>In) or technetium-99m exametazime (<sup>99m</sup>Tc). Each of these radionuclides has certain advantages, but ultimately the choice of which one to use is based on availability and personal preference. When cells are labeled with <sup>111</sup>In, imaging is performed 18-30 hours after infusion of labeled leukocytes, at which time the normal distribution of activity is limited to the liver, spleen and bone marrow (Figure 4)<sup>10</sup>.

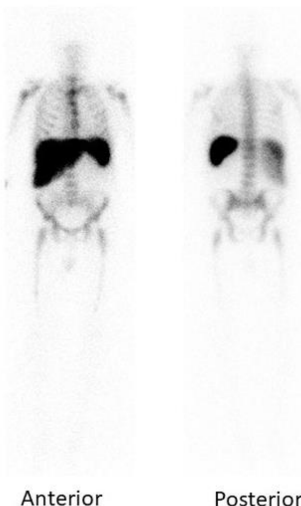


Figure 4. Normal indium-111 labeled leukocyte scan (24 hours post injection). Activity is confined to liver, spleen, and bone marrow.

When the cells are labeled with  $^{99m}\text{Tc}$ , imaging usually is performed within a few hours after labeled leukocyte reinfusion, although next day imaging is sometimes performed. The normal distribution of  $^{99m}\text{Tc}$ -WBC's is more variable than that of  $^{111}\text{In}$ -WBC's, because the bond between the

cell and the radionuclide is not as strong and consequently  $^{99m}\text{Tc}$  elutes out of the cells. In addition to the reticuloendothelial system, activity usually is present in the urinary tract, large bowel (by four hours after reinfusion) and occasionally the gall bladder (Figure 5)<sup>10</sup>.

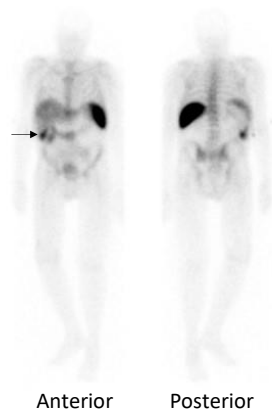


Figure 5. Normal technetium-99m labeled leukocyte scan (4 hours post injection). In addition to activity in the liver, spleen, and bone marrow, activity is present in the colon, urinary bladder and gall bladder (arrow).

Labeled leukocytes do not usually accumulate in tumors or in normally healing surgical incisions, which is an advantage over  $^{67}\text{Ga}$  and  $^{18}\text{F}$ -FDG<sup>10</sup>.

The role of WBC imaging in musculoskeletal infection has been extensively investigated. In one meta-analysis  $^{111}\text{In}$ -WBC imaging had a pooled sensitivity of 74% and a pooled specificity of 68% for diabetic pedal osteomyelitis<sup>11</sup>. In another meta-analysis the pooled sensitivities of  $^{99m}\text{Tc}$ -WBC and  $^{111}\text{In}$ -WBC scintigraphy were similar 91% versus 92%, respectively, but the pooled specificity of  $^{99m}\text{Tc}$ -WBC scintigraphy was higher, 92% vs. 75%<sup>12</sup>.

Initial reports of WBC imaging for lower extremity periprosthetic joint infections (PJI) were variable, with some investigations finding that the test was sensitive but not specific and others finding that it was specific but not sensitive. Poor sensitivity was hypothesized to be due to the chronicity of the infection i.e., neutrophilic migration had waned by the time the patient was imaged. However, neutrophils are invariably present in PJI, regardless of the duration. Poor specificity was attributed to nonspecific inflammation. Neutrophils typically are not part of the cellular response in aseptic periprosthetic joint inflammation, so inflammation

was not a good explanation for lack of specificity<sup>13</sup>. Subsequent investigations found that the inconsistent results reported were due to the variable distribution of the labeled leukocytes in the bone marrow. Leukocytes normally accumulate in the active reticuloendothelial component of the bone marrow, which in adults is assumed to be limited to the axial skeleton and proximal humeri and femurs. The distribution of active bone marrow is very variable and is affected by numerous conditions, both systemic and local, leading to generalized and focal bone marrow expansion, altering the "normal" distribution of the marrow, and making it difficult to differentiate labeled leukocyte accumulation in infection from accumulation in unusually located, but otherwise normal marrow. Differentiating labeled leukocyte accumulation in aberrant but otherwise normal marrow from accumulation in infection is accomplished by performing bone marrow imaging with  $^{99m}\text{Tc}$ -sulfur colloid. Leukocytes and sulfur colloid both accumulate in the reticuloendothelial cells of the bone marrow. The distribution of activity on labeled leukocyte and bone marrow images is similar in normal individuals and in individuals with underlying marrow

abnormalities, except for osteomyelitis, which stimulates uptake of leukocytes and suppresses uptake of sulfur colloid. In other words, in osteomyelitis the distribution of activity on the WBC and bone marrow images is different (Figure 6)<sup>14</sup>. In a systematic review that included 351 hip arthroplasties the pooled sensitivity of WBC/bone marrow imaging was 69%, 95% CI: 58%- 79%, and

the specificity was 96%, 95% CI: 93%-98%<sup>15</sup>. In a systematic review that included 144 knee arthroplasties pooled sensitivity was 80%, 95% CI: 66%-91%, and pooled specificity was 93%, 95% CI: 86%- 97%<sup>16</sup>. It should be noted that WBC/ marrow imaging is useful in virtually any condition that alters the distribution of bone marrow<sup>13</sup>.

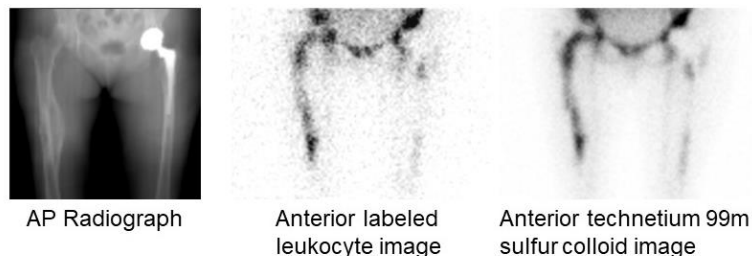


Figure 6. Uninfected fracture right femur. There is irregularly increased labeled leukocyte accumulation in the right femur, which could be interpreted as osteomyelitis. The distribution of activity on the bone marrow image (right) is virtually identical. The activity on the labeled leukocyte image is due to marrow, not infection. Note that the distribution of activity around the left hip replacement is similar on both images, again reflecting marrow not infection.

Labeled leukocyte imaging is not useful for diagnosing spondylodiscitis. For reasons that have yet to be elucidated, in 50% or more of the cases, spinal infection presents as nonspecific *decreased*, rather than increased uptake, which can be seen in numerous conditions besides infection<sup>8</sup>.

Labeled leukocyte imaging also is useful in cardiovascular infections. This test is a useful

adjunct in patients with suspected infective endocarditis, especially those involving prosthetic valves (Figure 7)<sup>17,18</sup>. In one investigation WBC SPECT/CT was 90% sensitive and 100% specific for infective endocarditis and was particularly useful in patients who were classified as possible infective endocarditis by the Dukes Criteria<sup>17</sup>.

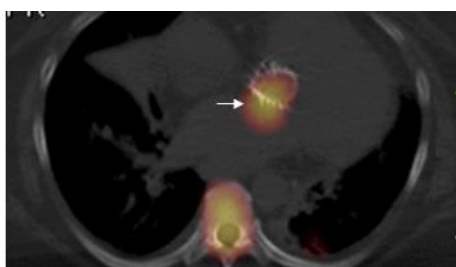


Figure 7. Infected prosthetic aortic valve with aortic root abscess. Axial SPECT/CT demonstrates intense uptake of indium-111 labeled leukocytes around the valve extending into the aortic root (arrow). Transesophageal echocardiogram performed 5 days earlier was negative.

When performed as SPECT/CT, WBC imaging is useful for confirming the presence of cardiac implantable device infection, defining extent of infection, and detecting complications. A negative study excludes infection with a high degree of certainty. Imaging the whole body, rather than just

the chest detects distant foci of infection and can identify alternative causes of infection<sup>19,20</sup>.

The sensitivity of WBC imaging for prosthetic vascular graft infection exceeds 90% in most investigations and is not affected by antibiotic

therapy or duration of symptoms. Specificity is more variable, ranging from about 50% to 100%<sup>10</sup>. The accuracy of the test is improved by performing SPECT/CT. In one investigation SPECT/CT was

100% accurate for diagnosing infection and was useful for detecting, localizing, and defining the extent of infection (Figure 8)<sup>21</sup>.

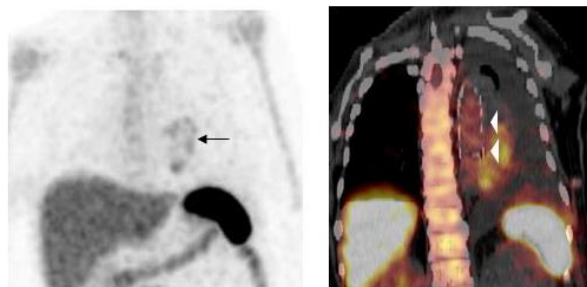


Figure 8. Infected aortic graft. Note the increased labeled leukocyte uptake in the left chest (arrow) on the maximum intensity projection (left). On the coronal SPECT/CT image (right), this activity is within the aortic graft (arrowheads).

Although CT is the imaging test of choice in the diagnostic workup of intrabdominal infections, WBC imaging has an important, adjunctive role in the workup of these infections. The test is sensitive and specific for intraabdominal infections such as abscesses and urinary tract infections<sup>22-24</sup>. In one investigation, both positive and negative results

provided useful information for patient management<sup>25</sup>. Furthermore labeled leukocytes do not accumulate in normally healing incisions or in uninfected tumors, which are important advantages over both <sup>67</sup>Ga and <sup>18</sup>F-FDG (Figure 9)<sup>10</sup>.

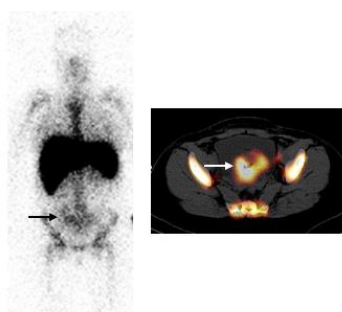


Figure 9. Endometritis. On the anterior indium-111 labeled leukocyte image (left) there is faintly increased labeled leukocyte activity in the pelvis (arrow). On the axial SPECT/CT image (right) there is increased activity throughout much of the uterus (arrow). An infected uterus with abscess formation was removed at surgery. The patient had undergone Caesarean section two weeks previously. CT scan (not shown) was inconclusive.

To capitalize on the advantages of positron emission tomography (PET), labeling leukocytes with PET compounds has been investigated. Leukocytes have been labeled in-vitro with <sup>18</sup>F-FDG, copper-64, and zirconium-89<sup>25-28</sup>. There are limitations inherent to all these agents, however, and it is not certain that any of them will become commercially available. It is also important to remember that, regardless of the radiolabel used, although WBC imaging is specific for leukocyte mediated inflammation, it is not specific for infection.

There are disadvantages to the in-vitro labeling procedure, regardless of the radiolabel used. The process is labor intensive, not always available, and requires direct contact with blood products. Labeling enough leukocytes to obtain diagnostically useful images in severely leukopenic individuals and in young children may not be possible. In-vivo methods of labeling leukocytes, primarily with antigranulocyte antibodies and antibody fragments, have been investigated. At the present time only one of these agents is still commercially available, a murine monoclonal G1

immunoglobulin,  $^{99m}\text{Tc}$ -besilesomab, which binds to Nonspecific Cross-reactive Antigen-95 present on neutrophils. The high incidence of dose-dependent human antimurine antibody response is a significant disadvantage to this agent because patients must be prescreened for the antibody and should not undergo repeat administration<sup>29</sup>.

### $^{18}\text{F}$ -FDG

With the rapid proliferation of clinical PET around the turn of the century, interest in positron emitting radiopharmaceuticals for diagnosing infection soon developed. PET provides high-resolution three-dimensional images of the whole body, which facilitates precise localization of radiopharmaceutical uptake, especially when performed as PET/CT. Semiquantitative analysis potentially could differentiate infectious from non-infectious conditions and be used to monitor response to treatment.

The first and most extensively investigated PET compound for imaging infection was  $^{18}\text{F}$ -FDG. Although developed and used primarily for tumor imaging, uptake of this radiopharmaceutical in inflammatory conditions was a well-known phenomenon that could confound study interpretation in patients with known or suspected malignancy. While this could be a disadvantage in patients with malignant disease, the potential of  $^{18}\text{F}$ -FDG for imaging inflammation and infection was exploited<sup>30</sup>.

There are three principal mechanisms that govern uptake cellular uptake of  $^{18}\text{F}$ -FDG: passive diffusion, active transport by a Na<sup>+</sup>-dependent glucose transporter (GLUT) and via GLUT-1 through GLUT-13 transporters. It is trapped intracellularly and does not diffuse back into the extracellular space<sup>31</sup>. Uptake of  $^{18}\text{F}$ -FDG in infection is related to leukocyte activation caused by the inflammatory process. The number and expression of glucose transporters and their affinity for deoxyglucose increase in activated inflammatory cells<sup>32</sup>. The  $^{18}\text{F}$ -FDG molecule is small and enters poorly perfused areas rapidly, so imaging can be performed within one to two hours after administration. Skeletal uptake usually normalizes within three to four months after trauma or surgery and degenerative bone changes usually show only mildly increased uptake, which are advantages in musculoskeletal infections<sup>33</sup>.

Imaging is performed one-two hours after radiopharmaceutical administration. The normal distribution of  $^{18}\text{F}$ -FDG includes the brain, myocardium, and urinary tract. Thymic uptake is sometimes seen, especially in children. Gastric and bowel activity are variable. Liver, spleen and bone marrow uptake generally are low-grade (Figure 10)<sup>33</sup>.

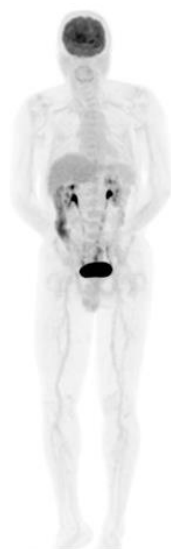


Figure 10. Normal  $^{18}\text{F}$ -FDG maximum intensity projection image. There is brain, myocardial, urinary tract, and colonic activity. Faint bone marrow activity also is present.



$^{18}\text{F}$ -FDG has become a valuable addition to molecular imaging in musculoskeletal infection, especially infections of the spine (Figure 11). In one meta-analysis, pooled sensitivity and specificity of  $^{18}\text{F}$ -FDG PET/PET-CT were 97% and 88%, respectively<sup>34</sup>. In another, pooled sensitivity and specificity were 94.8% and 91.4%, respectively<sup>35</sup>. In comparative investigations,  $^{18}\text{F}$ -FDG has outperformed bone and  $^{67}\text{Ga}$  scintigraphy<sup>36,37</sup>.

In a meta-analysis of  $^{18}\text{F}$ -FDG for diagnosing postoperative spinal infection, the summary AUC was 0.92 in patients with versus 0.98 in patients without spinal hardware. False positives were more frequent in patients with than in patients without hardware, 12.8% vs. 7%. Performing PET/CT rather than PET alone and analyzing uptake patterns can decrease hardware-associated false-positive results<sup>34,38</sup>.



Figure 11. Spondylodiscitis. There is focally increased  $^{18}\text{F}$ -FDG uptake in the mid thoracic spine (arrow) on the coronal PET/CT image.

This radiopharmaceutical is also useful in the diagnosis of diabetic foot osteomyelitis. In one meta-analysis the pooled sensitivity and specificity of  $^{18}\text{F}$ -FDG were 74% and 91%, respectively<sup>39</sup>. In another meta-analysis the pooled sensitivity and specificity for diagnosing diabetic foot osteomyelitis were 89% and 92% respectively, similar to what was reported for  $^{99\text{m}}\text{Tc}$ -WBC scintigraphy: 91% and 92%, respectively<sup>40</sup>. These data suggest that, although the results of both tests are comparable, given its advantages,  $^{18}\text{F}$ -FDG, if available, is preferable.

The role of  $^{18}\text{F}$ -FDG for diagnosing lower extremity periprosthetic joint infection has been extensively investigated. In one meta-analysis, pooled sensitivity and specificity of  $^{18}\text{F}$ -FDG-PET for diagnosing periprosthetic hip infection were 86% and 93%, respectively. The test was significantly more specific than bone scintigraphy and significantly more sensitive than combined WBC/bone marrow imaging.<sup>15</sup> In another meta-

analysis, pooled sensitivity and specificity were both 88%<sup>40</sup>. In yet another meta-analysis, pooled sensitivity and specificity were 83% and 90%, respectively<sup>41</sup>.

In a meta-analysis of periprosthetic knee infection, the pooled sensitivity and specificity of  $^{18}\text{F}$ -FDG were 70% and 84%, respectively<sup>16</sup>. In another, pooled sensitivity and specificity were 72% and 80% respectively<sup>42</sup>. In a third meta-analysis, pooled sensitivity and specificity were 90% and 75%, respectively<sup>41</sup>. In spite of these results, the role of  $^{18}\text{F}$ -FDG for diagnosing periprosthetic infection remains to be established<sup>13</sup>. Different test probabilities, an inability, to consistently discriminate between infection and aseptic inflammation, and an absence of standardized interpretative criteria remain obstacles to incorporating  $^{18}\text{F}$ -FDG into the routine diagnostic imaging workup for periprosthetic joint infection. (Figure 12)<sup>43</sup>.



Figure 12. Uninfected bilateral knee replacements. There is intense periprosthetic uptake around the right knee prosthesis and to a lesser extent, around the left knee replacement on the coronal  $^{18}\text{F}$ -FDG PET/CT image.

Published data indicate that  $^{18}\text{F}$ -FDG is of value for diagnosing cardiovascular infections. The test is a useful adjunct for diagnosing infective endocarditis

with a pooled sensitivity and specificity of 61% and 88%, respectively. It is especially useful in patients with prosthetic heart valves (Figure 13).

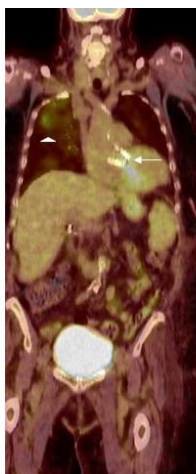


Figure 13. Infected prosthetic aortic valve (arrow). Note the  $^{18}\text{F}$ -FDG accumulation in the right upper lung (arrowhead), which was unsuspected pneumonia. This would not have been diagnosed on echocardiography.

False negative studies are associated with lesions below the limits of resolution of current systems and antibiotic treatment for more than one week prior to imaging. Postoperative inflammation during the first two months after implantation as well as prosthetic valve thrombosis are associated with false positive results. Compared to WBC imaging,  $^{18}\text{F}$ -FDG is more sensitive but less specific. It has been suggested that WBC imaging be reserved for situations in which  $^{18}\text{F}$ -FDG is inconclusive and during the first two months after surgery<sup>44,45</sup>.

Published data confirm that  $^{18}\text{F}$ -FDG is useful for diagnosing cardiac implantable device infections. This test accurately diagnoses and determines the extent of left ventricular assist device infections and improves the diagnostic accuracy of the modified Dukes Criteria (Figure 14)<sup>46-49</sup>.



Figure 14. Infected Cardiac Defibrillator. The abnormal  $^{18}\text{F}$ -FDG activity is confined to the pocket (arrow). The device and leads were removed, and the infection was confined to the pocket; the leads were not involved.

In a meta-analysis of nearly five hundred patients, the pooled sensitivity and specificity of  $^{18}\text{F}$ -FDG PET/CT for diagnosing these infections were 83% and 89%, respectively. Pooled sensitivity and specificity were 96% and 97%, respectively for pocket infection. The test was less sensitive for lead infection and cardiac implantable device infection with infective endocarditis with pooled sensitivity and specificity of 76% and 83%, respectively<sup>50</sup>. In a meta-analysis comparing  $^{18}\text{F}$ -FDG PET/CT and WBC SPECT/CT, pooled sensitivity and specificity of  $^{18}\text{F}$ -FDG PET-CT were 87% and 94%, respectively. There were insufficient data to perform a

meta-analysis for WBC SPECT/CT, but in the studies included, sensitivity exceeded 90% and specificity was 100%<sup>51</sup>.

The sensitivity and specificity of  $^{18}\text{F}$ -FDG for prosthetic vascular graft infection range from 88-100%<sup>52,53</sup>. Like any foreign body, prosthetic vascular grafts can incite an inflammatory reaction, which can lead to increased  $^{18}\text{F}$ -FDG activity, even in the absence of infection. Familiarity with normal  $^{18}\text{F}$ -FDG uptake patterns around these grafts and those associated with foreign body reaction and infection improves the accuracy of test (Figure 15)<sup>54-57</sup>.

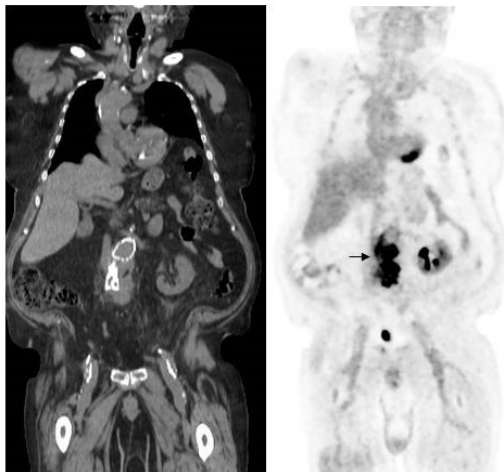


Figure 15. Infected abdominal aortic endovascular stent. Note the irregular, intense  $^{18}\text{F}$ -FDG uptake in the stent (arrow).

Data indicate that WBC SPECT/CT is superior to  $^{18}\text{F}$ -FDG for diagnosing prosthetic vascular graft infections. In a meta-analysis the pooled sensitivities of  $^{18}\text{F}$ -FDG PET/CT and WBC SPECT/CT were 95% and 99%, respectively. The pooled specificities were 80% and 82%, respectively. WBC SPECT/CT had a positive post-test probability of 96% and  $^{18}\text{F}$ -FDG PET/CT had a positive post-test probability of 83%<sup>58</sup>. In a prospective investigation of 39 patients,

with suspected infection of 96 prosthetic vascular grafts, the sensitivity, specificity, and accuracy of  $^{18}\text{F}$ -FDG PET/CT were 85%, 68.4% and 71.9%, respectively. Sensitivity, specificity, and accuracy of WBC SPECT/CT scan were 89.5%, 90.9%, and 90.6%, respectively. Interobserver agreement was good for  $^{18}\text{F}$ -FDG PET/CT: kappa value of 0.76, and excellent for WBC SPECT/CT: kappa value of 0.97<sup>59</sup>.

In a brief period of time,  $^{18}\text{F}$ -FDG has become the molecular imaging study of choice for sarcoid, with an overall sensitivity of 89%-100% (Figure 16). It is more sensitive than the ACE and Soluble

interleukin-2 receptor test. Whole-body imaging facilitates identification of unsuspected sites of disease, guiding patient management<sup>60,61</sup>.

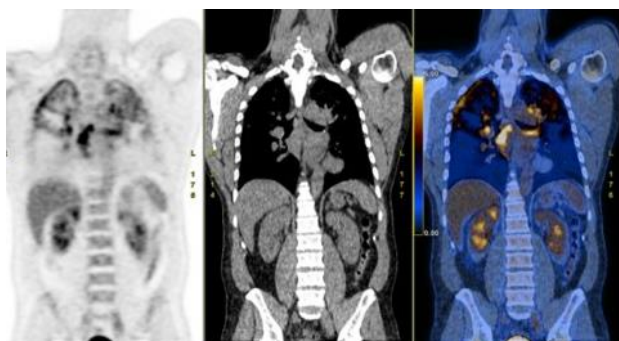


Figure 16. There is bilateral upper lung and mediastinal nodal uptake of  $^{18}\text{F}$ -FDG in a patient with active sarcoid.

This test is useful for monitoring treatment response (Figure 17). Decreasing  $^{18}\text{F}$ -FDG lesion avidity after initiating treatment correlates with

clinical improvement, while persistent activity is present in non-responders<sup>62,63</sup>.

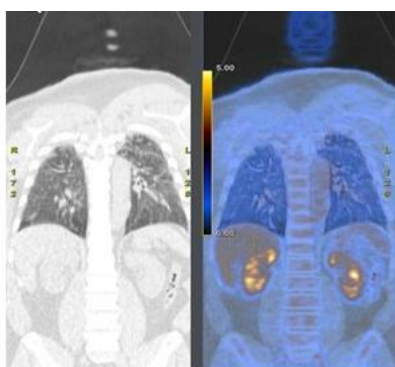


Figure 17. Follow up  $^{18}\text{F}$ -FDG after treatment shows complete resolution of the parenchymal and nodal abnormalities. (compare with figure 16)

Pulmonary parenchymal uptake correlates with active pulmonary disease and predicts response to anti-inflammatory treatment<sup>64</sup>. The differentiation between pure fibrosis and fibrosis plus inflammation is facilitated with  $^{18}\text{F}$ -FDG, which is superior to high resolution CT and serological evaluation for this purpose<sup>65,66</sup>. This is an important distinction,

because the presence of active inflammation might necessitate changes in therapy.

In patients with sarcoid,  $^{18}\text{F}$ -FDG has emerged as an important modality, with a sensitivity and specificity of 89% and 78%, respectively, for diagnosis (Figure 18)<sup>67</sup>.

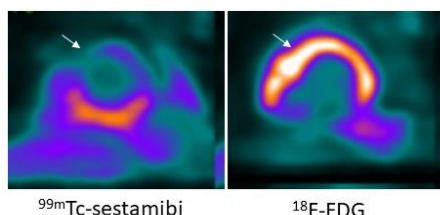


Figure 18. Cardiac sarcoid. On the myocardial perfusion image (left), there is a defect (arrow) in the mid anterior wall of the left ventricle. On the  $^{18}\text{F}$ -FDG image (right), there is increased activity (arrow) in the same region. This pattern is virtually diagnostic of cardiac sarcoid.

Quantification of myocardial  $^{18}\text{F}$ -FDG uptake is useful for assessing the severity of myocardial inflammation, and monitoring response to therapy<sup>68</sup>. A decrease in myocardial uptake on serial studies correlates with improved left ventricular ejection fraction<sup>69</sup>. A lack of decreased uptake on serial scans correlates with a significant increase in death, hospitalization for heart failure, heart transplantation, and ICD therapies<sup>70</sup>. Serial studies are useful for guiding immuno-suppressive therapy<sup>71</sup>.

In patients with tuberculosis,  $^{18}\text{F}$ -FDG is useful for identifying both pulmonary and extrapulmonary disease, measuring disease activity, identifying individuals with latent tuberculous infection at risk of developing active infection, and monitoring response to treatment<sup>72</sup>. Lesion activity correlates with disease activity. Using dual time-point imaging at one and two hours, it may be possible to distinguish active from inactive disease<sup>73</sup>. Even when radiological features may remain unchanged, early treatment response can be assessed with  $^{18}\text{F}$ -

FDG, significantly affecting patient management. In one investigation,  $^{18}\text{F}$ -FDG-PET/CT performed after two months of treatment, was the best method for early prediction of treatment results and long-term outcome<sup>74</sup>.

The workup of the patient with fever of unknown origin, or FUO, consists of first line investigations including history and physical examination, laboratory tests, chest x-ray, and echocardiography. When these investigations fail to yield a diagnosis, second-line tests including CT, MRI, and molecular imaging studies are performed. At one time the mainstays of molecular imaging for FUO,  $^{67}\text{Ga}$  and WBC imaging have been replaced by  $^{18}\text{F}$ -FDG as the molecular imaging test of choice for this entity in both adults and children (Figure 19).

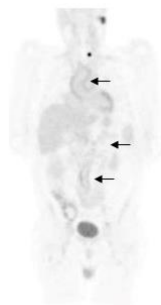


Figure 19. Vasculitis. There is diffusely increased  $^{18}\text{F}$ -FDG activity throughout the aorta (arrows). Vasculitis is a well-recognized cause of fever of unknown origin in the elderly.  $^{18}\text{F}$ -FDG is very sensitive for detecting large-vessel vasculitis and has shown promise for monitoring treatment response

A positive result contributes useful information by identifying the etiology of the fever and/or guiding further management, while a negative result excludes focal disease as the cause of the fever. A negative result also is a good predictor of a favorable prognosis. Performed early in the FUO workup,  $^{18}\text{F}$ -FDG PET/CT is cost effective by reducing the number of diagnostic procedures performed, obtaining a diagnosis sooner, and decreasing the number of undiagnosed cases<sup>75</sup>. A recent consensus panel recommended that  $^{18}\text{F}$ -FDG-PET/CT is an important diagnostic test after a patient fulfills FUO criteria with few or no diagnostic clues<sup>76</sup>.

## The Future

### INFECTION SPECIFIC AGENTS

Molecular imaging of infection has made great strides over the past five decades, beginning with  $^{99\text{m}}\text{Tc}$ -labeled diphosphonates and  $^{67}\text{Ga}$ , followed by labeled leukocytes and, more recently  $^{18}\text{F}$ -FDG, all of which contribute to detection of infection and help guide treatment. They have one limitation in common: they reflect the host response to infection, not the infection itself and therefore none of them are specific for infection. They cannot consistently differentiate infections from other

diseases and considerable effort has been devoted to developing infection specific imaging probes.

One of the earliest attempts to develop an infection specific molecular imaging agent was radiolabeled ciprofloxacin. The concept was that the radiolabeled antibiotic would be incorporated into bacteria, and foci of uptake on images would reflect infection. Although early data suggested that radiolabeled ciprofloxacin was sensitive and specific for infection, later investigations failed to confirm specificity and, at least briefly, enthusiasm for radiolabeled antibiotics as infection specific imaging agents faded<sup>29</sup>. Accumulation of <sup>18</sup>F-fluoropropyl-trimethoprim in *S. aureus*, *E. coli* and *P. aeruginosa* in-vitro has been demonstrated and in a murine myositis model, this agent localized sites of bacterial infection with *E. coli* and *S. aureus* and differentiated infection from sterile inflammation and tumor<sup>77</sup>. More recent data, using carbon-11 labeled trimethoprim, demonstrated the feasibility of imaging sensitive and drug resistant bacterial infections in humans<sup>78</sup>.

Antimicrobial peptides are an important component of the natural defenses of most living organisms. Most are small, cationic and amphipathic and have broad-spectrum activity against Gram-positive and Gram-negative bacteria, yeasts, fungi and viruses. They also have a role in apoptosis, wound healing, and immune modulation. Their expression may be constant or induced on contact with microbes and they may be transported by leukocytes to foci of infection. An important feature of antimicrobial peptides is that while they destroy microbes, they are not harmful to mammalian cells<sup>79</sup>. Radiolabeled synthetic fragments of a murine antimicrobial peptide ubiquicidin (UBI), have been investigated as infection specific imaging agents. Several investigations have reported that <sup>99m</sup>Tc- UBI-29-41 is both sensitive and specific for infection and is potentially useful for monitoring response to treatment<sup>80</sup>. A meta-analysis reported that pooled sensitivity, specificity and accuracy were 94.5%, 92.7%, and 93.7%<sup>81</sup>.

More recent investigations have used UBI fragments labeled with the PET agent, gallium-68. The results of preclinical investigations demonstrated sufficient-high target-to-background ratios to support further clinical development. Initial results in humans, though encouraging, are extremely limited<sup>82</sup>. No large-scale clinical trials of any radiolabeled antimicrobial peptides have ever been conducted.

The potential of radiolabeled sugars, other than <sup>18</sup>F-FDG, as infection specific molecular imaging agents has been studied. Radiolabeled trehalose analogs show potential as mycobacteria-specific imaging agents<sup>83</sup>. Preliminary data suggest that <sup>18</sup>F- labeled maltohexose is sensitive and specific for bacterial infection and can identify drug resistance in bacteria in vivo<sup>84</sup>.

Sorbitol, which is a sugar alcohol, is a metabolic substrate for Enterobacteriaceae. Radiolabeled sorbitol has been investigated as a bacteria specific molecular imaging agent<sup>85</sup>. In a murine model, <sup>18</sup>F-fluorodeoxysorbitol (<sup>18</sup>F-FDS), rapidly differentiated infection from sterile inflammation. <sup>18</sup>F-FDS also monitored the efficacy of antimicrobial treatment<sup>86</sup>. In an investigation that included 26 subjects <sup>18</sup>F-FDS PET/CT detected multiple sites of enterobacteriales infections. There was no correlation between the peripheral white blood cell or neutrophil counts and <sup>18</sup>F-FDS uptake in infected patients, which suggests that the uptake of this radiopharmaceutical does not depend on host inflammatory cells. In contrast to the intense uptake in foci of infection uptake in aseptic inflammation and tumors was minimal. Thirteen of the subjects with infection underwent repeat imaging after completion of treatment. In subjects who demonstrated clinical improvement, there was a significant decrease in uptake, while in subjects who failed to demonstrate clinical improvement, uptake did not decrease, suggesting that <sup>18</sup>F-FDS potentially could be used to monitor treatment response<sup>87</sup>.

Fungal infections have become a significant public health challenge because of increasing numbers of immunocompromised individuals. Although positive

cultures are the gold standard for diagnosis, the procedures for obtaining samples are invasive and are hampered by poor sensitivity and long turnaround times<sup>88</sup>. Noninvasive diagnostic procedures that are both sensitive and specific for fungal infection would be particularly useful. Even though <sup>18</sup>F-FDG cannot differentiate fungal from other infections or tumor, it has been used to monitor treatment response in patients with invasive fungal infections<sup>89</sup>. Radiolabeled monoclonal antibodies have also been investigated. The potential of copper-64-hJF5 for diagnosing invasive pulmonary aspergillosis has been investigated in patients with acute myeloid leukemia. In patients with infection, increased pulmonary uptake was observed, while in patients without infection, there was no pulmonary uptake of the agent<sup>90</sup>. Other agents under investigation include radiolabeled peptides and small proteins, chitin, which is a component of the fungal cell wall, and antifungal drugs<sup>88</sup>.

## Monitoring Treatment Response

Although treatment response is critical to the successful management of infectious diseases, there are controversies about reliable biomarkers for noninvasively gauging treatment response. The success, or failure, of treatment is usually based on a patient's subjective clinical response. Molecular imaging permits in vivo, noninvasive, quantitative assessment of biologic processes and has the potential to provide objective measurement of a patient's response to treatment. The history of monitoring treatment response with molecular imaging can be traced back to AIDS patients, when <sup>67</sup>Ga was used for monitoring treatment response and served as a prognosticator: a normal scan of the chest in an AIDS patient presenting with clinical progression of respiratory disease portended a grave prognosis. The significance of this was not fully appreciated at the time and until recently there were few investigations on the role of molecular imaging for monitoring treatment response and prognosis. There is a growing body of evidence indicating that <sup>18</sup>F-FDG is useful for monitoring treatment response and can provide prognostic information.

In one study, 90 sarcoidosis patients with persistent symptoms underwent <sup>18</sup>F-FDG PET/CT. The investigators found that <sup>18</sup>F-FDG PET/CT is a useful adjunct to other diagnostic methods for detecting active inflammatory sites, especially in patients with normal ACE levels. The test was advantageous for determining the extent of disease and influencing changes in therapy<sup>62</sup>. In a prospective study 27 sarcoidosis patients underwent two <sup>18</sup>F-FDG PET/CT scans one before and another at the end of therapy. Fourteen of the 27 patients were <sup>18</sup>F-FDG responders and 13 patients were non-responders. Although there was no difference in the clinical remission rates among responders, the relapse rate was significantly higher in non-responders than responders: 61.5% vs. 14.2%,  $p=0.018$ <sup>63</sup>. In another investigation, thirty patients with chronic sarcoidosis and active inflammation on baseline <sup>18</sup>F-FDG PET/CT underwent follow-up studies 12 months after treatment to evaluate response to treatment. Changes in uptake correlated with patients' own perceived changes in clinical symptoms. The authors concluded that <sup>18</sup>F-FDG PET/CT detects clinically meaningful changes in inflammatory activity in patients being treated for active chronic sarcoidosis and is a valuable adjunct to clinical evaluation for monitoring treatment<sup>91</sup>.

In patients with cardiac sarcoid, decreasing myocardial uptake on serial studies correlates with improved left ventricular ejection fraction, while a lack of decreased uptake correlates with a significant increase in deaths, hospitalizations for heart failure, heart transplantations, and ICD therapies<sup>69,70</sup>. Serial studies are useful for guiding immuno-suppressive therapy. In one study, 128 <sup>18</sup>F-FDG-PET scans were performed on thirty-four patients. Ninety-four scans, 73%, led to a change in therapy, including 42 that were instrumental for tapering prednisone. Over a median follow-up of 2.3 years, 48% of patients were successfully weaned from prednisone completely, and 20% were weaned to a maintenance dosage of 5-10mg/day<sup>71</sup>.

In patients with tuberculosis, <sup>18</sup>F-FDG can assess early treatment response when radiological

features may remain unchanged, significantly affecting patient management. In one series,  $^{18}\text{F}$ -FDG-PET/CT performed after two months of treatment, was the best method for early prediction of treatment results and long-term outcome<sup>74</sup>.

In patients with FUO, a negative  $^{18}\text{F}$ FDG result has prognostic value. In one investigation, 15 of 21 patients with FUO and a negative  $^{18}\text{F}$ -FDG PET/CT had spontaneous resolution of fever, with no evidence of an inflammatory, infectious, or malignant process during follow-up of up to three years<sup>92</sup>. In a meta-analysis, patients with negative  $^{18}\text{F}$ -FDG PET/CT results had a significantly higher likelihood of spontaneous remission than those with positive results,  $p < .001$ <sup>93</sup>.

Data on  $^{18}\text{F}$ -FDG imaging for monitoring treatment response in musculoskeletal infections has been limited almost exclusively to patients with spinal infections. In a prospective investigation 30 patients with spinal infection underwent  $^{18}\text{F}$ -FDG PET/CT before and after treatment. The change in SUVmax between the initial and follow up studies was the best predictor of residual infection<sup>94</sup>. In another prospective investigation,  $^{18}\text{F}$ -FDG PET/CT was used for early evaluation of response to antibiotic therapy in 34 patients with hematogenous spinal infection. Baseline study activity was compared to activity on the follow up study which was performed two to four weeks after the start of treatment. In responders  $^{18}\text{F}$ -FDG uptake was significantly less than on the baseline study<sup>95</sup>. In a retrospective investigation  $^{18}\text{F}$ -FDG-PET/CT scans were performed on 34 patients before and after at least 2 weeks of antibiotic therapy. Uptake decreased significantly in patients with clinical improvement, but in patients with disease progression<sup>96</sup>.

Some investigators report that  $^{18}\text{F}$ -FDG uptake patterns can be used to differentiate patients with active infection from those without active infection and patients who had a successful response to therapy. In 28 patients with spinal infection, non/poor responders had persistent  $^{18}\text{F}$ -FDG uptake in bone and soft tissue, while uptake

confined to the margins of a destroyed disc after treatment most likely represented mechanically induced inflammation rather than infection<sup>97</sup>.

## Conclusions

Molecular imaging of infection and inflammation has come a long way over the past fifty years, starting with  $^{99\text{m}}\text{Tc}$  diphosphonates and  $^{67}\text{Ga}$ , progressing to labeled leukocytes and more recently,  $^{18}\text{F}$ -FDG. These agents have made significant contributions to detection of infection, and in some cases, helped guide treatment. Future investigations should focus on the development of specific probes for imaging infections, delineating the extent of the infection and monitoring treatment response.

## Conflict of Interest:

None.

## Funding Statement:

None.

## Acknowledgements:

None.



## References:

1. Ordonez AA, Sellmyer MA, Gowrishankar G, et al. Molecular imaging of bacterial infections: Overcoming the barriers to clinical translation. *Sci Transl Med.* 2019;11(508):eaax8251. doi: 10.1126/scitranslmed.aax8251.
2. Palestro CJ. Radionuclide imaging of musculoskeletal infection: A review. *J Nucl Med.* 2016;57(9):1406-12. doi: 10.2967/jnumed.115.157297.
3. Schauwecker DS. The scintigraphic diagnosis of osteomyelitis. *AJR Am J Roentgenol.* 1992;158(1):9-18. doi: 10.2214/ajr.158.1.1727365.
4. Lavender JP, Lowe J, Barker JR, Burn JI, Chaudhri MA. Gallium 67 citrate scanning in neoplastic and inflammatory lesions. *Br J Radiol.* 1971 May;44(521):361-6. doi: 10.1259/0007-1285-44-521-361.
5. Deysine M, Robinson R, Rafkin H, Teicher I, Silver L, Aufses AH Jr. Clinical infections detected by 67Ga scanning. *Ann Surg* 1974;80(6):897-901. doi: 10.1097/00000658-197412000-00018.
6. Palestro CJ. The current role of gallium imaging in infection. *Semin Nucl Med.* 1994;24(2):128-41. doi: 10.1016/s0001-2998(05)80227-2.
7. Palestro CJ, Metter D. Molecular imaging of inflammation and infection. In Ahmadzadehfar H, Biersack HJ, Freeman LM, Zuckier LS (editors): *Clinical Nuclear Medicine 2nd ed*; Switzerland: Springer Nature, 2020:511-537.
8. Raghavan M, Palestro CJ. Imaging of spondylodiscitis: An update. *Semin Nucl Med.* 2023;53(2):152-166. doi: 10.1053/j.semnuclmed.2022.11.005.
9. Thakur ML, Lavender JP, Arnot RN, Silvester DJ, Segal AW. Indium-111-labeled autologous leukocytes in man. *J Nucl Med.* 1977 Oct;18(10):1014-21.
10. Palestro CJ, Love C, Bhargava KK. Labeled leukocyte imaging: current status and future directions. *Q J Nucl Med Mol Imaging.* 2009;53(1):105-23. PMID: 19182734.
11. Johnson JE, Kennedy EJ, Shereff MJ, Patel NC, Collier BD. Prospective study of bone, indium-111-labeled white blood cell, and gallium-67 scanning for the evaluation of osteomyelitis in the diabetic foot. *Foot Ankle Int.* 1996;17(1):10-6. doi: 10.1177/107110079601700103.
12. Lauri C, Tamminga M, Glaudemans AWJM, et al. Detection of osteomyelitis in the diabetic foot by imaging techniques: A systematic review and meta-analysis comparing MRI, white blood cell scintigraphy, and FDG-PET. *Diabetes Care.* 2017; 40(8):1111-1120. doi: 10.2337/dc17-0532.
13. Palestro CJ. Molecular imaging of periprosthetic joint infections. *Semin Nucl Med.* 2023;53(2):167-174. doi: 10.1053/j.semnuclmed.2022.11.004.
14. Palestro CJ, Love C, Tronco GG, Tomas MB, Rini JN. Combined labeled leukocyte and technetium 99m sulfur colloid bone marrow imaging for diagnosing musculoskeletal infection. *RadioGraphics.* 2006;26(3):859-70. doi: 10.1148/rg.263055139.
15. Verberne SJ, Raijmakers PG, Temmerman OP. The accuracy of imaging techniques in the assessment of periprosthetic hip infection: A systematic review and meta-analysis. *J Bone Joint Surg Am.* 2016;98(19):1638-1645. doi: 10.2106/JBJS.15.00898.
16. Verberne SJ, Sonnega RJ, Temmerman OP, Raijmakers PG. What is the accuracy of nuclear imaging in the assessment of periprosthetic knee infection? A meta-analysis. *Clin Orthop Relat Res.* 2017;475(5):1395-1410. doi: 10.1007/s11999-016-5218-0.
17. Erba PA, Conti U, Lazzeri E, et al. Added value of 99mTc-HMPAO-labeled leukocyte SPECT/CT in the characterization and management of patients with infectious endocarditis. *J Nucl Med.* 2012;53(8):1235-43. doi: 10.2967/jnumed.111.099424.
18. Hyafil F, Rouzet F, Lepage L, et al. Role of radiolabelled leucocyte scintigraphy in patients with a suspicion of prosthetic valve endocarditis and inconclusive echocardiography. *Eur Heart J Cardiovasc Imaging.* 2013;14(6):586-94. doi: 10.1093/ehjci/jet029.
19. Erba PA, Sollini M, Conti U, et al. Radiolabeled WBC scintigraphy in the diagnostic workup of

- patients with suspected device-related infections. *JACC Cardiovasc Imaging*. 2013;6(10):1075-1086. doi: 10.1016/j.jcmg.2013.08.001.
20. Litzler PY, Manrique A, Etienne M, et al. Leukocyte SPECT/CT for detecting infection of left-ventricular-assist devices: preliminary results. *J Nucl Med*. 2010;51(7):1044-8. doi: 10.2967/jnumed.109.070664.
21. Erba PA, Leo G, Sollini M, Tascini C, et al. Radiolabelled leucocyte scintigraphy versus conventional radiological imaging for the management of late, low-grade vascular prosthesis infections. *Eur J Nucl Med Mol Imaging*. 2014 Feb; 41(2):357-68. doi: 10.1007/s00259-013-2582-9.
22. Lantto EH, Lantto TJ, Vorne M. Fast diagnosis of abdominal infections and inflammations with technetium-99m-HMPAO labeled leukocytes. *J Nucl Med*. 1991;32(11):2029-34. PMID: 1941134.
23. Rypins EB, Evans DG, Hinrichs W, Kipper SL. Tc-99m-HMPAO white blood cell scan for diagnosis of acute appendicitis in patients with equivocal clinical presentation. *Ann Surg*. 1997; 226(1):58-65. doi: 10.1097/0000658-199707000-00008.
24. Baba AA, McKillop JH, Cuthbert GF, Neilson W, Gray HW, Anderson JR. Indium 111 leucocyte scintigraphy in abdominal sepsis. Do the results affect management? *Eur J Nucl Med*. 1990;16(4-6):307-9. doi: 10.1007/BF00842785.
25. Rini JN, Palestro CJ. Imaging of infection and inflammation with 18F-FDG-labeled leukocytes. *Q J Nucl Med Mol Imaging*. 2006;50(2):143-6.
26. Bhargava KK, Gupta RK, Nichols KJ, Palestro CJ. In vitro human leukocyte labeling with (64)Cu: an intraindividual comparison with (111)In-oxine and (18)F-FDG. *Nucl Med Biol*. 2009 Jul;36(5):545-9. doi: 10.1016/j.nucmedbio.2009.03.001.
27. Fairclough M, Prenant C, Ellis B, et al. A new technique for the radiolabelling of mixed leukocytes with zirconium-89 for inflammation imaging with positron emission tomography. *J Labelled Comp Radiopharm*. 2016;59(7):270-6. doi: 10.1002/jlcr.3392.
28. Kahts M, Guo H, Kommidi H, et al. 89Zr-leukocyte labelling for cell trafficking: in vitro and preclinical investigations. *EJNMMI Radiopharm Chem*. 2023;8(1):36. doi: 10.1186/s41181-023-00223-1.
29. Palestro CJ, Glaudemans AWJM, Dierckx RAJO. Multiagent imaging of inflammation and infection with radionuclides. *Clin Transl Imaging*. 2013;1(6):385-396. doi: 10.1007/s40336-013-0041-z.
30. Zhuang H, Alavi A. 18-fluorodeoxyglucose positron emission tomographic imaging in the detection and monitoring of infection and inflammation. *Semin Nucl Med*. 2002;32(1):47-59. doi: 10.1053/snuc.2002.29278.
31. Meller J, Sahlmann CO, Scheel AK. 18F-FDG PET and PET/CT in fever of unknown origin. *J Nucl Med*. 2007;48(1):35-45. PMID: 17204697.
32. Palestro CJ. FDG-PET in musculoskeletal infections. *Semin Nucl Med*. 2013;43(5):367-76. doi: 10.1053/j.semnuclmed.2013.04.006.
33. Love C, Tomas MB, Tronco GG, Palestro CJ. FDG PET of infection and inflammation. *Radiographics*. 2005;25(5):1357-68. doi: 10.1148/rg.255045122.
34. Prodromou ML, Ziakas PD, Poulou LS, Karsaliakos P, Thanos L, Mylonakis E. FDG PET is a robust tool for the diagnosis of spondylodiscitis: a meta-analysis of diagnostic data. *Clin Nucl Med*. 2014;39:330-335. DOI: 10.1097/RLU.0000000000000336.
35. Treglia G, Pascale M, Lazzeri E, van der Bruggen W, Delgado Bolton RC, Glaudemans AWJM. Diagnostic performance of 18F-FDG PET/CT in patients with spinal infection: a systematic review and a bivariate meta-analysis. *Eur J Nucl Med Mol Imaging*. 2020;47:1287-1301. DOI: 10.1007/s00259-019-04571-6.
36. Gratz S, Dörner J, Fischer U, et al. 18F-FDG hybrid PET in patients with suspected spondylitis. *Eur J Nucl Med Mol Imaging*. 2002;29(4):516-24. doi: 10.1007/s00259-001-0719-8.
37. Fuster D, Solà O, Soriano A, et al. A prospective study comparing whole-body FDG PET/CT to combined planar bone scan with 67Ga SPECT/CT in the Diagnosis of Spondylodiskitis.

- Clin Nucl Med.* 2012;37(9):827-32. doi: 10.1097/RLU.0b013e318262ae6c.
38. Bagrosky BM, Hayes KL, Koo PJ, Fenton LZ. 18F-FDG PET/CT evaluation of children and young adults with suspected spinal fusion hardware infection. *Pediatr Radiol.* 2013;43(8):991-1000. doi: 10.1007/s00247-013-2654-9.
39. Treglia G, Sadeghi R, Annunziata S, et al. Diagnostic performance of Fluorine-18-Fluorodeoxyglucose positron emission tomography for the diagnosis of osteomyelitis related to diabetic foot: a systematic review and a meta-analysis. *Foot (Edinb).* 2013;23(4):140-8. doi: 10.1016/j.foot.2013.07.002.
40. Lauri C, Tamminga M, Glaudemans AWJM, et al. Detection of osteomyelitis in the diabetic foot by imaging techniques: A systematic review and meta-analysis comparing MRI, white blood cell scintigraphy, and FDG-PET. *Diabetes Care.* 2017 Aug;40(8):1111-1120. doi: 10.2337/dc17-0532. PMID: 28733376.
41. Kwee TC, Kwee RM, Alavi A. FDG-PET for diagnosing prosthetic joint infection: systematic review and metaanalysis. *Eur J Nucl Med Mol Imaging.* 2008;35:2122–2132. doi:10.1007/s00259-008-0887-x.
42. Jin H, Yuan L, Li C, Kan Y, Hao R, Yang J. Diagnostic performance of FDG PET or PET/CT in prosthetic infection after arthroplasty: a meta-analysis. *Q J Nucl Med Mol Imaging.* 2014;58(1):85-93. PMID: 24469570.
43. Pinski JM, Chen AF, Estok DM, Kavolus JJ. Nuclear medicine scans in total joint replacement. *J Bone Joint Surg Am.* 2021;103(4):359-372. doi: 10.2106/JBJS.20.00301.
44. Yan J, Zhang C, Niu Y, et al. The role of 18F-FDG PET/CT in infectious endocarditis: a systematic review and meta-analysis. *Int J Clin Pharmacol Ther.* 2016;54(5):337-42. doi: 10.5414/CP202569.
45. Rouzet F, Chequer R, Benali K, et al. Respective performance of 18F-FDG PET and radiolabeled leukocyte scintigraphy for the diagnosis of prosthetic valve endocarditis. *J Nucl Med.* 2014 Dec;55(12):1980-5. doi: 10.2967/jnumed.114.141895.
46. Pizzi MN, Roque A, Fernández-Hidalgo N, et al. Improving the diagnosis of infective endocarditis in prosthetic valves and intracardiac devices with 18F-fluorodeoxyglucose positron emission tomography/computed tomography angiography: Initial results at an infective endocarditis referral center. *Circulation.* 2015;132(12):1113-26. doi: 10.1161/CIRCULATIONAHA.115.015316.
47. Bensimhon L, Lavergne T, Hugonnet F, et al. Whole body [(18) F]fluorodeoxyglucose positron emission tomography imaging for the diagnosis of pacemaker or implantable cardioverter defibrillator infection: a preliminary prospective study. *Clin Microbiol Infect.* 2011;17(6):836-44. doi: 10.1111/j.1469-0691.2010.03312.x.
48. Sarrazin JF, Philippon F, Tessier M, et al. Usefulness of fluorine-18 positron emission tomography/computed tomography for identification of cardiovascular implantable electronic device infections. *J Am Coll Cardiol.* 2012;59(18):1616-25. doi: 10.1016/j.jacc.2011.11.059.
49. Dell'Aquila AM, Mastrobuoni S, Alles S, et al. Contributory role of fluorine 18-fluorodeoxyglucose positron emission tomography/computed tomography in the diagnosis and clinical management of infections in patients supported with a continuous-flow left ventricular assist device. *Ann Thorac Surg.* 2016;101(1):87-94; discussion 94. doi: 10.1016/j.athoracsur.2015.06.066.
50. Mahmood M, Kendi AT, Farid S, et al. Role of 18F-FDG PET/CT in the diagnosis of cardiovascular implantable electronic device infections: A meta-analysis. *J Nucl Cardiol.* 2019;26(3):958-970. doi: 10.1007/s12350-017-1063-0.
51. Juneau D, Golfam M, Hazra S, et al. Positron emission tomography and single-photon emission computed tomography imaging in the diagnosis of cardiac implantable electronic device infection: A systematic review and meta-analysis. *Circ Cardiovasc Imaging.* 2017;10(4):e005772. doi: 10.1161/CIRCIMAGING.116.005772.

52. Keidar Z, Engel A, Hoffman A, Israel O, Nitecki S. Prosthetic vascular graft infection: the role of 18F-FDG PET/CT. *J Nucl Med.* 2007;48(8):1230-6. doi: 10.2967/jnumed.107.040253.
53. Sah BR, Husmann L, Mayer D, et al. Diagnostic performance of 18F-FDG-PET/CT in vascular graft infections. *Eur J Vasc Endovasc Surg.* 2015;49(4):455-64. doi: 10.1016/j.ejvs.2014.12.024.
54. Keidar Z, Pirmisashvili N, Leiderman M, Nitecki S, Israel O. 18F-FDG uptake in noninfected prosthetic vascular grafts: incidence, patterns, and changes over time. *J Nucl Med.* 2014;55(3):392-5. doi: 10.2967/jnumed.113.128173.
55. Saleem BR, Pol RA, Slart RH, Reijnen MM, Zeebregts CJ. 18F-Fluorodeoxyglucose positron emission tomography/CT scanning in diagnosing vascular prosthetic graft infection. *Biomed Res Int.* 2014;2014:471971. doi: 10.1155/2014/471971.
56. Bennett P, Tomas MB, Koch CF, Nichols KJ, Palestro CJ. Appearance of aseptic vascular grafts after endovascular aortic repair on [(18)F]fluorodeoxyglucose positron emission tomography/computed tomography. *World J Radiol.* 2023;15(8):241-249. doi: 10.4329/wjr.v15.i8.241.
57. Bowles H, Ambrosioni J, Mestres G, et al. Diagnostic yield of 18F-FDG PET/CT in suspected diagnosis of vascular graft infection: A prospective cohort study. *J Nucl Cardiol.* 2020;27(1):294-302. doi: 10.1007/s12350-018-1337-1.
58. Reinders Folmer EI, Von Meijenfildt GCI, et al. Diagnostic imaging in vascular graft infection: A systematic review and meta-analysis. *Eur J Vasc Endovasc Surg.* 2018;56(5):719-729. doi: 10.1016/j.ejvs.2018.07.010.
59. Puges M, Bérard X, Ruiz JB, et al. Retrospective study comparing WBC scan and 18F-FDG PET/CT in patients with suspected prosthetic vascular graft infection. *Eur J Vasc Endovasc Surg.* 2019;57(6):876-884. doi: 10.1016/j.ejvs.2018.12.032.
60. Keijsers RGM, Grutters JC. In which patients with sarcoidosis is FDG PET/CT indicated? *J Clin Med.* 2020;9(3):890. doi: 10.3390/jcm9030890.
61. Akaike G, Itani M, Shah et al. PET/CT in the diagnosis and workup of sarcoidosis: focus on atypical manifestations. *Radiographics.* 2018;38(5):1536-49. doi: 10.1148/rg.2018180053.
62. Sobic-Saranovic D, Grozdic I, Videnovic-Ivanov J, et al. The utility of 18F-FDG PET/CT for diagnosis and adjustment of therapy in patients with active chronic sarcoidosis. *J Nucl Med.* 2012;53:1543-9. doi: 10.2967/jnumed.112.104380.
63. Maturu VN, Rayamajhi SJ, Agarwal R, Aggarwal AN, Gupta D, Mittal BR. Role of serial F-18 FDG PET/CT scans in assessing treatment response and predicting relapses in patients with symptomatic sarcoidosis. *Sarcoidosis Vasc Diffuse Lung Dis.* 2016;33(4):372-80.
64. Keijsers RG, Verzijlbergen JF, van Diepen DM, van den Bosch JM, Grutters JC. 18F-FDG PET in sarcoidosis: an observational study in 12 patients treated with infliximab. *Sarcoidosis Vasc Diffuse Lung Dis.* 2008;25(2):143-9.
65. Guleria R, Jyothidasan A, Madan K, et al. Utility of FDG-PET-CT scanning in assessing the extent of disease activity and response to treatment in sarcoidosis. *Lung India.* 2014;31(4):323-30. doi: 10.4103/0970-2113.142092.
66. Mostard RL, Vöö S, van Kroonenburgh MJ, et al. Inflammatory activity assessment by F18 FDG-PET/CT in persistent symptomatic sarcoidosis. *Respir Med.* 2011;105(12):1917-24. doi: 10.1016/j.rmed.2011.08.012.
67. Youssef G, Leung E, Mylonas I, et al. The use of 18F-FDG PET in the diagnosis of cardiac sarcoidosis: a systematic review and metaanalysis including the Ontario experience. *J Nucl Med.* 2012;53:241-8. doi: 10.2967/jnumed.111.090662.
68. Chareonthaitawee P, Beanlands RS, Chen W, et al. Joint SNMMI-ASNC expert consensus document on the role of 18F-FDG PET/CT in cardiac sarcoid detection and therapy monitoring. *J Nucl Cardiol.* 2017;24(5):1741-58. doi: 10.1007/s12350-017-0978-9.
69. Osborne MT, Hulten EA, Singh A, et al. Reduction in <sup>18</sup>F-fluorodeoxyglucose uptake on

- serial cardiac positron emission tomography is associated with improved left ventricular ejection fraction in patients with cardiac sarcoidosis. *J Nucl Cardiol.* 2014;21(1):166-74. doi: 10.1007/s12350-013-9828-6.
70. Muser D, Santangeli P, Castro SA, et al. Prognostic role of serial quantitative evaluation of 18F-fluorodeoxyglucose uptake by PET/CT in patients with cardiac sarcoidosis presenting with ventricular tachycardia. *Eur J Nucl Med Mol Imaging.* 2018;45(8):1394-1404. doi: 10.1007/s00259-018-4001-8.
71. Ning N, Guo HH, Iagaru A, Mittra E, Fowler M, Witteles R. Serial cardiac FDG-PET for the diagnosis and therapeutic guidance of patients with cardiac sarcoidosis. *J Card Fail.* 2019;25(4):307-11. doi: 10.1016/j.cardfail.2019.02.018.
72. Soussan M, Brillet PY, Mekinian A, Khafagy A, Nicolas P, Vessieres A, et al. Patterns of pulmonary tuberculosis on FDG-PET/CT. *Eur J Radiol.* 2012;81(10):2872-6. doi: 10.1016/j.ejrad.2011.09.002.
73. Kim IJ, Lee JS, Kim SJ, et al. Double-phase 18F-FDG PET-CT for determination of pulmonary tuberculoma activity. *Eur J Nucl Med Mol Imaging.* 2008;35(4):808-14. doi: 10.1007/s00259-007-0585-0.
74. Chen RY, Dodd LE, Lee M, et al. PET/CT imaging correlates with treatment outcome in patients with multidrug-resistant tuberculosis. *Sci Transl Med.* 2014;6(265):265ra166. doi: 10.1126/scitranslmed.3009501.
75. Palestro CJ, Brandon DC, Dibble EH, Keidar Z, Kwak JJ. FDG PET in evaluation of patients with fever of unknown origin: AJR expert panel narrative review. *AJR Am J Roentgenol.* 2023;221(2):151-162. doi: 10.2214/AJR.22.28726.
76. Wright WF, Stelmash L, Betrains A, et al. Recommendations for updating fever and inflammation of unknown origin from a modified Delphi consensus panel. *Open Forum Infect Dis.* 2024;11(7):ofae298. doi: 10.1093/ofid/ofae298.
77. Sellmyer MA, Lee I, Hou C, et al. Bacterial infection imaging with [18F]fluoropropyl-trimethoprim. *Proc Natl Acad Sci U S A.* 2017;114(31):8372-8377. doi: 10.1073/pnas.1703109114.
78. Lee IK, Jacome DA, Cho JK, et al. Imaging sensitive and drug-resistant bacterial infection with [11C]-trimethoprim. *J Clin Invest.* 2022;132(18):e156679. doi: 10.1172/JCI156679.
79. Wang G. Human antimicrobial peptides and proteins. *Pharmaceuticals (Basel).* 2014;7(5):545-94. doi: 10.3390/ph7050545.
80. Lupetti A, Pauwels EK, Nibbering PH, Welling MM. 99mTc-antimicrobial peptides: promising candidates for infection imaging. *Q J Nucl Med.* 2003;47(4):238-45.
81. Ostovar A, Assadi M, Vahdat K, Nabipour I, Javadi H, Eftekhari M, et al. A pooled analysis of diagnostic value of 99mTc-Ubiquidin (UBI) scintigraphy in detection of an infectious process. *Clin Nucl Med.* 2013;38:413-6. doi: 10.1097/RLU.0b013e3182867d56.
82. Marjanovic-Painter B, Kleynhans J, Zeevaert JR, Rohwer E, Ebenhan T. A decade of ubiquidin development for PET imaging of infection: A systematic review. *Nucl Med Biol.* 2023;116-117:108307. doi: 10.1016/j.nucmedbio.2022.11.001.
83. Rundell SR, Wagar ZL, Meints LM, et al. Deoxyfluoro-d-trehalose (FDTre) analogues as potential PET probes for imaging mycobacterial infection. *Org Biomol Chem.* 2016;14(36):8598-609. doi: 10.1039/c6ob01734g.
84. Ning X, Seo W, Lee S, et al. PET imaging of bacterial infections with fluorine-18-labeled maltohexaose. *Angew Chem Int Ed Engl.* 2014;53(51):14096-101. doi: 10.1002/anie.201408533.
85. Ordonez AA, Jain SK. Pathogen-specific bacterial imaging in nuclear medicine. *Semin Nucl Med.* 2018;48(2):182-94. doi: 10.1053/j.semnuclmed.2017.11.003.
86. Weinstein EA, Ordonez AA, DeMarco VP, et al. Imaging enterobacteriaceae infection in vivo with 18F-fluorodeoxysorbitol positron emission tomography. *Sci Transl Med.* 2014;6(259):259ra146. doi: 10.1126/scitranslmed.3009815.

87. Ordonez AA, Wintaco LM, Mota F, et al. Imaging Enterobacterales infections in patients using pathogen-specific positron emission tomography. *Sci Transl Med*. 2021;13(589):eabe9805. doi: 10.1126/scitranslmed.abe9805.
88. Lai J, Wang B, Petrik M, Beziere N, Hammoud DA. Radiotracer development for fungal-specific imaging: Past, present, and future. *J Infect Dis*. 2023;228(Suppl 4):S259-S269. doi: 10.1093/infdis/jiad067.
89. Kim DY, Pyo A, Ji S, et al. In vivo imaging of invasive aspergillosis with 18F-fluorodeoxysorbitol positron emission tomography. *Nat Commun*. 2022;13(1):1926. doi: 10.1038/s41467-022-29553-5.
90. Davies G, Rolle AM, Maurer A, et al. Towards translational immune PET/MR imaging of invasive pulmonary aspergillosis: The humanised monoclonal antibody JF5 detects aspergillus lung infections in vivo. *Theranostics*. 2017;7(14):3398-414. doi: 10.7150/thno.20919.
91. Sobic-Saranovic DP, Grozdic IT, Videnovic-Ivanov J, et al. Responsiveness of FDG PET/CT to treatment of patients with active chronic sarcoidosis. *Clin Nucl Med*. 2013;38(7):516-21. doi: 10.1097/RLU.0b013e31828731f5.
92. Keidar Z, Gurman-Balbir A, Gaitini D, Israel O. Fever of unknown origin: the role of 18F-FDG PET/CT. *J Nucl Med*. 2008;49(12):1980-5. doi: 10.2967/jnumed.108.054692.
93. Takeuchi M, Nihashi T, Gafter-Gvili A, et al. Association of 18F-FDG PET or PET/CT results with spontaneous remission in classic fever of unknown origin: A systematic review and meta-analysis. *Medicine (Baltimore)*. 2018;97(43):e12909. doi: 10.1097/MD.00000000000012909. Kim SJ, Kim IJ, Suh KT, et al. Prediction of residual disease of spine infection using F-18 FDG PET/CT. *Spine*. 2009;34:2424-30.
94. Kim SJ, Kim IJ, Suh KT, et al. Prediction of residual disease of spine infection using F-18 FDG PET/CT. *Spine*. 2009;34:2424-30.
95. Nanni C, Boriani L, Salvadori C, et al. FDG PET/CT is useful for the interim evaluation of response to therapy in patients affected by haematogenous spondylodiscitis *Eur J Nucl Med Mol Imaging*. 2012;39:1538-44. doi: 10.1007/s00259-012-2179-8
96. Righi E, Carnelutti A, Muser D, et al. Incremental value of FDG-PET/CT to monitor treatment response in infectious spondylodiscitis. *Skeletal Radiol*. 2020;49:903-12. doi: 10.1007/s00256-019-03328-4.
97. Riccio SA, Chu AK, Rabin HR, et al. Fluorodeoxyglucose positron emission tomography/computed tomography interpretation criteria for assessment of antibiotic treatment response in pyogenic spine infection. *Can Assoc Radiol J*. 2015;66:145-52. doi: 10.1016/j.carj.2014.08.004.